

Mechanism of 2,5-Dioxopiperazine Formation

Sante Capasso,^{*,†,‡} Alessandro Vergara,[§] and Lelio Mazzarella^{†,§}

Contribution from the Centro di Studio di Biocristallografia, C.N.R., via Mezzocannone 4, 80134 Napoli, Italy, Facoltà di Scienze Ambientali, Seconda Università di Napoli, via Arena 22, 81100 Caserta, Italy, and Dipartimento di Chimica, Università di Napoli "Federico II", via Mezzocannone 4, 80134 Napoli, Italy

Received June 23, 1997

Abstract: The cyclization of H-Ala-Pro-NH₂ to the 2,5-dioxopiperazine (DKP) has been studied as a model for the spontaneous cleavage of the peptide bond with concomitant formation of 2,5-dioxopiperazine that can occur at the N-terminus of a polypeptide chain. The reaction involves pre-equilibrium attack of the N-terminal amino group on the carbonyl carbon of the second residue giving a zwitterionic cyclic intermediate, T[±], which is in acid–base equilibrium with various forms characterized by different grades of protonation, T⁰, T⁺ and T⁻. The Brønsted plot for the base-catalysis and the pH-rate profile give pK_a ~ 7 and ~ 13 for the equilibria T⁻ + H⁺ ⇌ T[±] and T⁻ + H⁺ ⇌ T⁰, respectively. The reaction is subject to general base and general acid catalysis, acting on different steps. Departure of the amino group from T⁰ and T⁻ by two parallel routes gives the product. The bifunctional acid catalyst HCO₃⁻ strongly increases the reaction rate and at high concentrations causes a change of the rate-limiting step. At high pH, the overall reaction rate is limited by the trans → cis isomerization of the Ala-Pro peptide bond.

Introduction

2,5-Dioxopiperazine (diketopiperazine, DKP) formation from the N-terminal residues of a peptide chain commonly occurs as a disturbing reaction in the synthesis¹ and long-term storage of peptides.^{2,3} In addition, many DKPs, encompassing a wide range of biological activities, have been found in a variety of tissues and body fluids.⁴ The nitrogen atom of the N-terminal deprotonated amino group can attack the carbonyl carbon atom of the second residue causing the breakdown of the chain and formation of DKPs.⁵ This reaction is known to occur easily in dipeptide esters⁶ because of the presence of good leaving groups (alcohol molecules) and in dipeptides with alternate chirality¹ because of the higher stability of the resulting DKPs. For D/L DKPs the amino acid side chains will lie on opposite sides of the plane of the cycle. As in the dioxopiperazine rings both peptide bonds must be in cis conformation, the cyclization reaction is promoted by N-alkylated cyclic residues in second position because of their high propensity to form a cis peptide bond with the preceding residue.^{7,8} The recent interest in the stability of N-alkylated residues^{3,9} is mainly due to their use in

the design of conformationally restricted cyclic peptides,¹⁰ to be employed in the study of structure–biological activity relationship.¹¹ Moreover, it has been suggested¹² that the posttranslational N-acetylation of proteins in higher organism is an evolutionary protection against spontaneous degradation via formation of DKPs.

The nucleophilic addition of amino groups to carbonyl carbon atoms has been the subject of extensive investigation, since it is involved in many reactions such as the formation of peptides, imines and so forth. It has been observed that the attack of the nitrogen atom on the carbonyl carbon usually occurs along a preferred direction,¹³ producing a zwitterionic unstable intermediate which, by acid–base reactions, gives intermediates with various grades of protonation.^{14–16} As concerns the formation of DKPs from the N-terminal residues of a polypeptide chain, the current literature mostly deals with the influence of acids and bases on the reaction occurring during peptide synthesis in organic solvents.¹⁷ Recently, an efficient novel route for the synthesis of DKPs on a solid support has been described.¹⁸ The

[†] Centro di Studio di Biocristallografia, C.N.R.

[‡] Seconda Università di Napoli.

[§] Università di Napoli "Federico II".

(1) Bodanszky, M. *Principles of Peptide Synthesis*; Springer-Verlag: Berlin, 1984; pp 158–201.

(2) (a) Battersby, J. E.; Hancock, W. S.; Canova-Davis, E.; Oeswein, J.; O'Connor, B. *Int. J. Peptide Prot. Res.* **1994**, *44*, 215–222. (b) Kertescher, U.; Bienert, M.; Krause, E.; Sepetov, N.; Mehli, B. *Int. J. Peptide Prot. Res.* **1993**, *41*, 207–211. (c) Steinberg, S.; Bada, J. L. *Science* **1981**, *213*, 544–545.

(3) Marsden, B. J.; Nguyen, T. M.-D.; Schiller, P. W. *Int. J. Peptide Prot. Res.* **1993**, *41*, 313–316.

(4) Mortier, J.; Chene, A.; Gelin, J.; Moyroud, J. *Tetrahedron* **1996**, *52*, 8525–8534.

(5) Møss, J.; Bundgaard, H. *J. Pharm. Pharmacol.* **1990**, *42*, 7–12.

(6) (a) Field, G. B.; Noble, R. L. *Int. J. Peptide Prot. Res.* **1990**, *35*, 161–214. (b) Beyermann, M.; Bienert, M.; Niedrich, H.; Carpino, L. A.; Sadat-Aalee, D. *J. Org. Chem.* **1990**, *55*, 721–728.

(7) (a) Stewart, D. E.; Sarkar, A.; Wampler, J. E. *J. Mol. Biol.* **1990**, *214*, 253–260. (b) Ramachandean, G. N.; Mitra, A. K. *J. Mol. Biol.* **1976**, *107*, 85–92.

(8) Grathwohl, C.; Wüthrich, K. *Biopolymers* **1976**, *15*, 2043–2057.

(9) Capasso, S.; Sica, F.; Mazzarella, L.; Balboni, G.; Guerrini, R.; Sanvadori, S. *Int. J. Peptide Prot. Res.* **1995**, *45*, 567–573.

(10) Toniolo, C. *Int. J. Peptide Prot. Res.* **1990**, *35*, 287–300.

(11) Lomize, A. L.; Pogozheva, I. D.; Mosberg, H. I. *Biopolymers* **1996**, *38*, 221–234.

(12) Radzicka, A.; Wolfenden, R. *J. Am. Chem. Soc.* **1996**, *118*, 6105–6109.

(13) (a) Dunitz, J. D. *X-ray analysis and the structure of organic molecules*; Cornell University Press: Ithaca and London, **1979**; pp 301–384. (b) Kirby, A. J. *Adv. Phys. Org. Chem.* **1994**, *29*, 87–183.

(14) (a) Jencks, W. P. *Acc. Chem. Res.* **1976**, *9*, 425–432. (b) Camilleri, P.; Ellul, R.; Kirby, A. J.; Mujahid, T. G. *J. Chem. Soc., Perkin Trans. 2* **1979**, 1617–1620.

(15) Kirby, A. J.; Mujahid, T. G.; Camilleri, P. *J. Chem. Soc., Perkin Trans. 2* **1979**, 1610–1616.

(16) Fox, J. P.; Jencks, W. P. *J. Am. Chem. Soc.* **1974**, *96*, 1436–1449.

reaction mechanism in water solution has never been studied, apart from a few reports concerning the catalytic effect of acids.^{4,9}

This paper reports a detailed kinetic study of the formation of 2,5-dioxopiperazine from H-Ala-Pro-NH₂ in water. In the selected peptide, the Pro should ensure a sufficiently high cyclization rate also at acidic pH. Furthermore, since in short peptides the trans ↔ cis isomerization of the X-Pro bond is relatively fast,^{19,20} this isomerization reaction is expected to be rate-limiting step only under conditions that strongly increase the rate of DKP formation.

Experimental Section

Materials. H-Ala-Pro-NH₂·HCl (**I**) was obtained from Bachem. Its apparent acid dissociation constant, K_a , was determined under the conditions of the kinetic experiments ($T = 20\text{ }^\circ\text{C}$, $\mu = 1\text{ M}$) by titration with 0.01 M KOH. The method of the half-neutralization point gave a pK_a of 7.8.

Ala-Pro 2,5-dioxopiperazine (**II**) was prepared by adding concentrated ammonia solution to a water solution of **I** (10 mg/mL) up to pH 10.0. After 1 day, acetic acid was added to bring the pH to neutrality. After lyophilization, purification was carried out by semipreparative HPLC on a C₁₈ column eluted with 0.1% (w/v) trifluoroacetic acid in water. Electrospray mass spectrum, recorded on a Bio-Q triple quadrupole instrument (Micromass, Manchester, U.K.), gave $MH^+ = 169$. ¹H NMR recorded in [D₂O]DMSO at 400 MHz gave δ = 1.20 (d, 3H, CH₃, Ala), 1.70–2.20 (m, 4H, C^βH₂-C^γH₂, Pro), 3.30–3.45 (m, 2H, C^αH₂, Pro), 4.00–4.10 (m, 2H, C^αH, Ala and C^αH, Pro), 8.20 (d, 1H, NH, Ala).

Kinetic Measurements. Water solutions of **I** (0.25 mM) at the desired pH and buffer concentration were filtered through a 0.45 μm membrane filter and then stored in a thermostatted bath at 20 ± 0.1 °C. At preselected times, an aliquot was removed and analyzed by HPLC on a Beckman model system gold using a Beckman C₈ reversed phase column (4.0 × 250 mm, 5 μm particle size) eluted with 0.1% (v/v) trifluoroacetic acid in 3% (v/v) acetonitrile in H₂O at a flow rate of 0.7 mL/min. Peptides were detected using a Beckman model 166 variable wavelength monitor at 214 nm with a Shimadzu C-R6A integrating recorder. The product of the reaction was identified by comparison with HPLC traces of authentic sample.

The following buffers were used in the concentration range of 50–200 mM: CH₃COOH/CH₃COO⁻, pH 3.9–5.3; cacodylic acid/cacodylate anion, pH 5.5–6.6; H₂PO₄⁻/HPO₄²⁻, pH 5.9–7.1; 2-methylimidazole hydrochloride/2-methylimidazole, pH 6.8–8.8; Tris⁺H⁺/Tris, pH 7.4–8.6; morpholine hydrochloride/morpholine, pH 8.2–9.3; HCO₃⁻/CO₃²⁻ (buffer concentration 20–400 mM), pH 9.2–10.4; ⁺NH₃-CH₂-CH₂-OH/NH₂-CH₂-CH₂-OH, pH 10.2–11.6. Dilute HCl and KOH were used in the pH ranges 2.5–3.1 and 12.1–13.8, respectively.

In all samples, a constant ionic strength of 1 M was maintained by the addition of an appropriate volume of a concentrate solution of KCl. The pH values were measured by glass electrode at the same temperature and ionic strength as those of the rate measurements.

The rate constants were calculated by least-squares analysis, assuming the rate of the cyclization reaction to be first-order in [**I**]. The fitting of the experimental data was satisfactory for all samples. The values of rate constants, obtained from different runs carried out under the same experimental conditions, were reproducible to within 10%, except at acidic pH where the lower value of the reaction rate ($t_{1/2}$ being on the order of a few months) resulted in a lower reproducibility.

The temperature effect on the reaction rate was analyzed performing kinetic runs in the range of 20–70 °C, 0.1 M phosphate buffer, pH 6.8 (measured at 20 °C), and calculating the preexponential factor and the

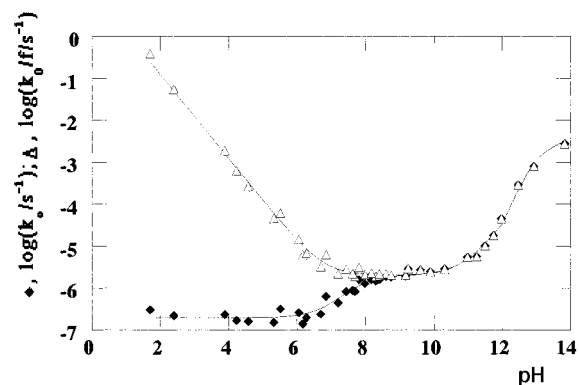


Figure 1. pH rate profile for the cyclization of H-Ala-Pro-NH₂ to the 2,5-dioxopiperazine at $T = 20\text{ }^\circ\text{C}$ and $\mu = 1\text{ M}$: on the ordinate ◆, $\log(k_0)$ and Δ, $\log(k_0/f)$, k_0 is the observed first-order rate constant extrapolated to zero buffer concentration, and f the fraction of H-Ala-Pro-NH₂ in the deprotonated form.

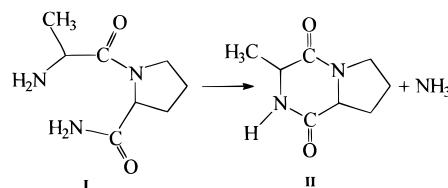
activation energy from the linear regression of $\ln(k)$ versus $1/T$ by least-squares method. The entropy and enthalpy of activation were calculated by the standard formulae derived from the absolute theory of reaction rates.²¹

Calculation of the pK_a Values of the Reaction Intermediates. The pK_a values for the equilibria $T^\pm + H^+ \rightleftharpoons T^+$ (pK_2) and $T^- + H^+ \rightleftharpoons T^0$ (pK_3) defined in Figure 7 were calculated by the procedure of Fox and Jencks,¹⁶ as $\Delta pK_a = \rho \sum \sigma_i$ relative to that of the parent compounds, using the ρ value of -9.1 ²² and the σ_i values derived by Hansch et al.²³ Starting from the parent compounds CH₃NH₂CH₂OH⁺ ($pK_a = 9.98$ for the proton of the hydroxyl group) and CH₃OH ($pK_a = 15.2$), we obtained the values of 8 and 13 for pK_2 and pK_3 respectively. pK_1 ($T^- + H^+ \rightleftharpoons T^\pm$) was obtained only by the Brønsted plots as reported in the Results section. pK_4 ($T^0 + H^+ \rightleftharpoons T^+$) was obtained by the equation $pK_4 = pK_1 + pK_2 - pK_3$.

Cis ↔ Trans Conformational Equilibrium. The percentage of *cis* isomer in H-Ala-Pro-NH₂ was determined in D₂O solution at pH 6.5, $\mu = 1\text{ M}$ KCl, by monodimensional proton NMR spectra recorded at 400 MHz on a Varian Unit 400 spectrometer, at 0.02 and 0.2 M phosphate. At both concentrations, the percentage of the *cis* isomer, determined by the ratio of the area of the Ala β-proton resonance of the two isomers, was about 13%, in excellent agreement with the results previously obtained by Grathwohl and Wüthrich⁸ on the same dipeptide in different conditions. These authors also showed that the deprotonation of the N-terminal amino group only slightly increases the fraction of the *cis* dipeptide.

Results

The cyclization rate of **I** to **II** exhibits a marked pH and buffer dependence and is pseudo-first-order in the starting peptide throughout the pH range explored. No hydrolysis of the DKP and/or that of the starting dipeptide has been detected.



pH Dependence of the Reaction Rate. Figure 1 shows a plot of $\log(k_0)$ versus pH, where k_0 is the observed first-order rate constant extrapolated to zero buffer concentration. k_0 is

(21) Connors, K. A. *Chemical Kinetics: The Study of Reaction Rates in Solution*; VCH Publishers: New York, 1990; pp 187–243.

(22) Taylor, P. J. *J. Chem. Soc., Perkin Trans. 2* **1993**, 1423–1427.

(23) Hansch, A.; Leo, H. A.; Taft, R. W. *Chem. Rev.* **1991**, *91*, 165–195.

(17) (a) Gisin, B. F.; Merrifield, R. B. *J. Am. Chem. Soc.* **1972**, *94*, 3102–3106. (b) Pedroso, E.; Grandas, A.; de las Heras, X.; Eritja, R.; Giralt, E. *Tetrahedron Lett.* **1986**, 743–746.

(18) Szardenings, A. K.; Burkoth, T. S.; Lu, H. H.; Tien, D. W.; Campbell, D. A. *Tetrahedron* **1997**, *53*, 6573–6593.

(19) Melander, W. R.; Jacobson, J.; Horvath, C. *J. Chromatogr.* **1982**, *234*, 269–276.

(20) Grathwohl, C.; Wüthrich, K. *Biopolymers* **1981**, *20*, 2623–2633.

pH independent at acidic pH, increases in the proximity of the pK_a of the conjugate acid of the N-terminal amino group ($pK_a = 7.8$) and for $pH > 11$, with an intermediate plateau. In the range of 11.0–12.0, $\log(k_o)$ linearly increases with unity slope, thereby indicating hydroxide ion catalysis. At higher pH the rate constant initially increases more rapidly and then gradually levels off with an inflection point at $pH \approx 13$, suggesting either the formation of an ionizable intermediate with a $pK_a \approx 13$ or a change of the rate-determining step, or a combination of both.²⁴

The pH dependence of the rate constant k_o up to $pH \approx 12.0$ is well approximated by

$$k_o = k_1 \left\{ \frac{10^{-pH}}{K_a + 10^{-pH}} \right\} + \{k_2 + k_{OH^-} [OH^-]\} \left\{ \frac{K_a}{K_a + 10^{-pH}} \right\} \quad (1)$$

where the apparent rate constants k_1 and k_2 take into account the uncatalyzed or water-catalyzed reaction of the protonated and neutral forms of **I**, respectively, k_{OH^-} is the catalytic constant for the hydroxide ion-catalyzed reaction of the neutral form, and K_a is the dissociation constant of the conjugate acid of **I**. The dotted lines, drawn in Figure 1 at pH value below 12.0, have been generated by this equation with the values $k_1 = 2.0 \times 10^{-7} \text{ s}^{-1}$, $k_2 = 2.1 \times 10^{-1} \text{ s}^{-1}$ and $k_{OH^-} = 2.5 \times 10^{-3} \text{ M s}^{-1}$ as obtained by least-squares analysis. The pH dependence of $\log(k_o)$ is similar to that previously observed for the formation of **DKP** from H-Tyr-Tic-Phe-Phe-NH₂ in the pH range of 4–9.⁹ In the latter reaction, the restricted pH range explored did not allow the determination of k_2 and k_{OH^-} , however, the value of k_1 ($7.9 \times 10^{-7} \text{ s}^{-1}$) is in good agreement with that obtained in the present work. For **DKP** formation from H-His-Pro-NH₂, a bell-shaped pH-rate profile centered at pH 6.5 has been reported that has been related to the acid–base equilibrium of the His residue.⁵ The experimental data reported here also suggest a close correlation between the studied reaction and the cyclization of 2-(aminomethyl)benzamide to phthalimidine.²⁵ In this molecule, the aromatic ring imposes a favorable geometry for the nucleophilic attack of the amino group on the carboxyl carbon atom of the amide group, similar to that imposed by the cis configuration of **I**. Indeed, the values of k_1 , k_2 , and k_{OH^-} normalized by 0.13, i.e., the fraction of **I** in the cis configuration as estimated by NMR spectra, are in good agreement with those reported for the cyclization of 2-(aminomethyl)benzamide to phthalimidine at neutral and basic pH values, particularly for k_1 ($4.0 \times 10^{-6} \text{ s}^{-1}$) and k_2 ($2.0 \times 10^{-5} \text{ s}^{-1}$). It should be noted, however, that the pH dependence of the reaction rate in the two cases is considerably different at acidic pH, suggesting that in this pH region the two reactions proceed through different routes.

In the reasonable hypothesis that **DKP** formation from peptides requires the N-terminal amino group to be in the unprotonated form, a more clear description of the pH dependence of the reaction rate can be obtained by plotting $\log(k_o/f)$ versus pH (see Figure 1), where f is the unprotonated fraction of the peptide at each pH. The expected linear dependence with slope -1 at acidic pH is a diagrammatic representation of the occurrence of hydronium catalysis in this pH region.

Buffer Catalysis. The pseudo-first-order rate constant (k_{obs}), determined at constant pH, increases monotonically with buffer concentration. Except for carbonate, the relationship is linear within the experimental errors, and the catalytic constant (k_{cat})

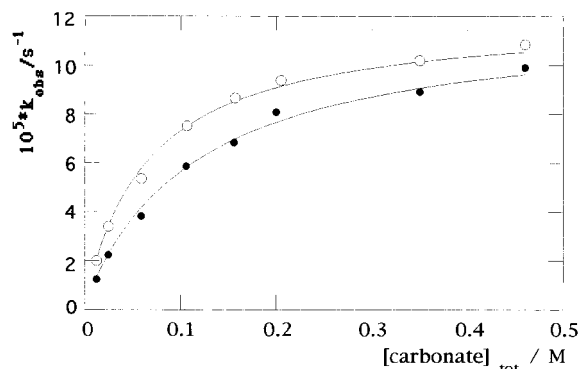


Figure 2. Dependence of the observed first-order rate constant (k_{obs}) for the cyclization of H-Ala-Pro-NH₂ to the 2,5-dioxopiperazine on the total carbonate buffer concentration at the fraction 0.2 (open symbols) and 0.8 (filled symbols) of free base.

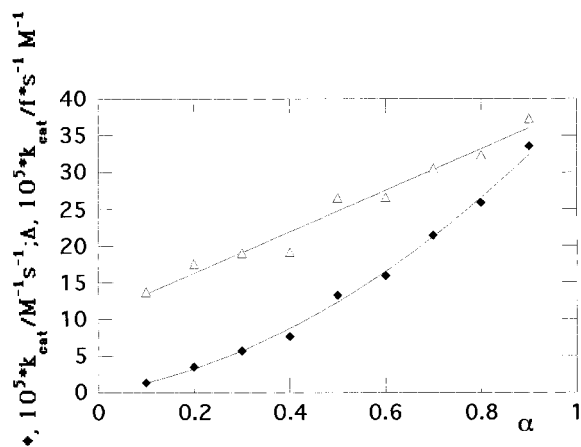


Figure 3. Plot of k_{cat} and k_{cat}/f for the cyclization of H-Ala-Pro-NH₂ to the 2,5-dioxopiperazine against the fraction (α) of the free base in the 2-methylimidazole hydrochloride/2-methylimidazole buffer: on the ordinate \blacklozenge , k_{cat} and \triangle , k_{cat}/f . k_{cat} is the catalytic constant of the buffers, and f is the fraction of the reactant in the deprotonated form.

of the buffer can be obtained from the slope of the regression. For the carbonate buffer, where the kinetic constant first increases rapidly at low concentrations of buffer and then gradually levels off at higher concentrations (Figure 2), k_{cat} was estimated at zero buffer concentration. For the basic buffers ($pK_a > 8.5$) morpholine, carbonate, and ethanolamine, the k_{cat} values change linearly with the fraction α of the buffer free bases. While for 2-methylimidazole, whose pK_a (7.8) is very close to that of the ammonium group of the substrate, the plot of k_{cat} versus α shows a very clear down curvature (Figure 3). To rationalize this dependence, the values of k_{cat} were divided at each pH by the fraction (f) of the peptide with the amino group in the deprotonated form. On the reasonable hypothesis that the buffer acts only on the deprotonated form, this ratio, k_{cat}/f , should represent the effective catalytic rate constant for the buffer. The plots of k_{cat}/f versus α , also shown in Figure 3, show a linear dependence. This is a clear indication that the buffer acts only on the neutral form of the substrate. The buffers Tris, phosphate, cocadylate, and acetate also show a down curvature in the $k_{cat} - \alpha$ plots, although for these buffers the deviation from a straight line are considerably less marked. Figure 4 shows the dependence of k_{cat}/f versus α for all buffers used except 2-methylimidazole, which is considered in Figure 3 (of course, for the basic buffers k_{cat}/f is practically coincident with k_{cat}): all curves are linear within the experimental errors. In these figures, the intercepts at $\alpha = 0$ and $\alpha = 1$ give a good estimate of the second-order rate constants for the acid- (k_{HA})

(24) Willi, A. V. *Comprehensive Chemical Kinetics*; Bamford, C. H., Tipper, C. F. H., Eds.; Elsevier: Amsterdam, 1977; Vol. 8, pp 1–95.

(25) Fife, T. H.; DeMark, B. R. *J. Am. Chem. Soc.* **1976**, *98*, 3075–3080.

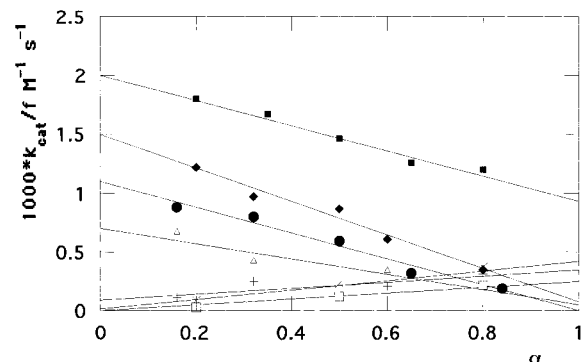


Figure 4. Plot of k_{cat}/f for the cyclization of H-Ala-Pro-NH₂ to the 2,5-dioxopiperazine against the fraction (α) of the free base in the buffers CH₃COOH/CH₃COO⁻ (●), cacodylic acid/cacodylate salt (◆), H₂PO₄⁻/HPO₄²⁻ (△), Tris·H⁺/Tris (+), morpholine hydrochloride/morpholine (×), HCO₃⁻/CO₃²⁻ (■), ⁺NH₃-CH₂-CH₂-OH/NH₂-CH₂-CH₂-OH (□). K_{cat} is the catalytic constant of the buffers, and f is the fraction of the reactant in the deprotonated form. For presentation purposes, the k_{cat}/f values of CH₃COOH/CH₃COO⁻ and H₂PO₄⁻/HPO₄²⁻ have been scaled down by a factor of 5.

Table 1. Second-Order Rate Constants for General Acid (k_{HA}) and General Base Catalysis (k_{B}) of Dioxopiperazine Formation from H-Ala-Pro-NH₂ at 20 °C and Ionic Strength 1.0 M^a

acid catalyst	k_{HA} (M ⁻¹ s ⁻¹)	k_{B} (M ⁻¹ s ⁻¹)
H ₃ O ⁺	12.6	
CH ₃ COOH	5.5×10^{-3}	1.5×10^{-5}
cacodylic acid	1.5×10^{-3}	7.6×10^{-5}
H ₂ PO ₄ ⁻	3.5×10^{-3}	2.5×10^{-4}
2-methylimidazole hydrochloride	1.0×10^{-3}	3.9×10^{-4}
Tris·H ⁺	8.7×10^{-5}	3.5×10^{-4}
morpholine hydrochloride	1.3×10^{-5}	4.2×10^{-4}
HCO ₃ ⁻	2.0×10^{-3}	9.3×10^{-4}
⁺ NH ₃ CH ₂ CH ₂ OH		2.5×10^{-4}
H ₂ O		2.5×10^{-3}

^a Estimate errors are less than 10%.

and base-catalyzed (k_{B}) reactions, respectively. Their values are reported in Table 1, together with the catalytic constants for the hydronium and hydroxide ion catalysis derived from the fit of eq 1. $k_{\text{H}_3\text{O}^+}$ is given by the apparent rate constant k_1 for the uncatalyzed reaction of the protonated form of **I** divided by the dissociation constant ($1 \times 10^{-7.8}$ M) of the conjugate acid of **I**.

In the hypothesis that the catalysts act only on unprotonated form of the peptide, the low value of k_{B} for the acetate buffer strongly suggests that the acetate catalysis mainly involves the acidic form of the buffer. On the other hand, the value of k_{HA} for ethanolamine, which has the highest $\text{p}K_{\text{a}}$ among the buffers used, is zero within the experimental error, indicating that only the basic form of this buffer acts as an efficient catalyst. A more quantitative correlation of k_{HA} and k_{B} with the $\text{p}K_{\text{a}}$ of the buffers (Brønsted plot) is shown in Figure 5. The values of k_{HA} for H₃O⁺, CH₃COOH, cacodylic acid, 2-methylimidazole hydrochloride, Tris·H⁺, and morpholine, fit well the linear correlation $\log k_{\text{HA}} = \log k_{\text{HA},0} - \alpha \text{p}K_{\text{a}}$, with $\alpha = 0.54 \pm 0.02$ (Brønsted coefficient); whereas for the polyfunctional catalyst HCO₃⁻ and, to a lesser extent, for H₂PO₄⁻, k_{HA} is greater than expected on the basis of this correlation. When the k_{HA} value for H₃O⁺ was not included in the computation, we obtained $\alpha = 0.60 \pm 0.02$ and $\log k_{\text{HA},0} = 0.7 \pm 0.2$.

With regard to the base catalysis, the relatively short range and the large errors of k_{B} values do not allow a clear-cut determination of the curve slopes. Nevertheless, a curve with unity slope up to $\text{p}K_{\text{a}} \approx 7$, followed by a region where $\log(k_{\text{B}})$

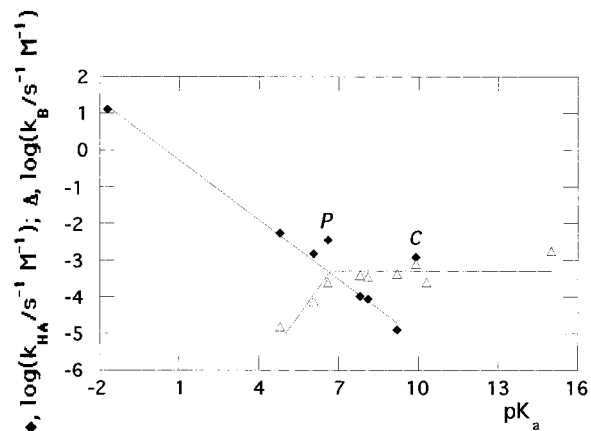


Figure 5. Brønsted plots for the cyclization of H-Ala-Pro-NH₂ to the 2,5-dioxopiperazine. On the ordinate: ◆, $\log(k_{\text{HA}})$ and △, $\log(k_{\text{B}})$. k_{HA} and k_{B} are the second-order rate constants for the acid and base catalysis, respectively. The usual statistical corrections have been applied for the phosphate and carbonate buffers. The letters P and C mark the points for the acid catalysis of H₂PO₄⁻ and HCO₃⁻, respectively.

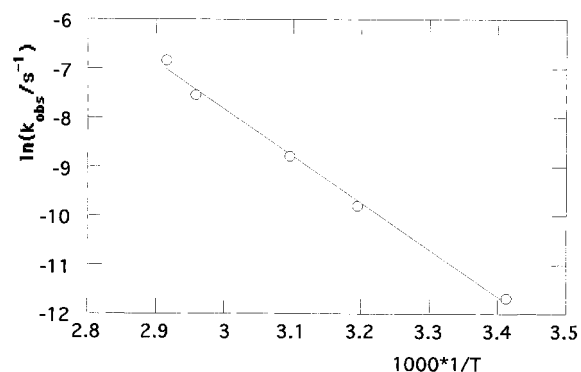


Figure 6. Arrhenius plot for the cyclization of H-Ala-Pro-NH₂ to the 2,5-dioxopiperazine in 0.1 M phosphate buffer, pH 7.8.

Table 2. Preexponential Factor and Apparent Activation Parameters for the Cyclization of H-Ala-Pro-NH₂ to the 2,5-Dioxopiperazine, Ionic Strength 1.0 M

A (s ⁻¹)	20 ± 2
E_{a} (kJ mol ⁻¹)	74 ± 6
ΔH^{\ddagger} (kJ mol ⁻¹)	71 ± 5
ΔS^{\ddagger} (J K ⁻¹ mol ⁻¹)	29 ± 2

is constant, seems a reasonable interpretation of the data. This shape of the Brønsted plot is indicative of a simple proton transfer from a reaction intermediate to the base catalyst, which occurs in the thermodynamically favorable direction (diffusion-controlled process) for buffers having $\text{p}K_{\text{a}}$ values of the conjugate acid greater than 7, and in the thermodynamically unfavorable direction for lower $\text{p}K_{\text{a}}$ values.^{26,27} From these considerations, the $\text{p}K_{\text{a}}$ of the intermediate can be estimated to be about 7.

Temperature Dependence of the Reaction Rate. The Arrhenius plot for the cyclization of **I** to **II**, determined in phosphate buffer, is linear in the temperature range studied (Figure 6). The preexponential factor and the apparent activation parameters are given in Table 2. The values of E_{a} and ΔH^{\ddagger} have been corrected by the heat of ionization of the dihydrogen phosphate (3.3 kJ mol⁻¹).²⁸

(26) Eigen, M. *Angew. Chem. Int. Ed. Engl.* **1964**, 3, 1–19.

(27) Hibbert, F. *Adv. Phys. Org. Chem.* **1986**, 22, 113–212.

(28) Connors, K. A. *Chemical Kinetics: The Study of Reaction Rates in Solution*; VCH Publishers: New York, 1990; pp 245–309.

Discussion

The salient features of the kinetic behavior of **DKP** formation that are informative on the reaction mechanism can be summarized as follows:

(a) The nonlinear dependence of the rate constant on the carbonate buffer concentration suggests the existence of an intermediate, the formation of which is rate determining at some catalyst concentrations, while, at others, the rate-limiting step is the conversion of intermediate to products.²⁹ Moreover, the limiting rate, reached at high carbonate concentration (pH range of 9.2–10.4), is surpassed at high pH, for instance k_0 at pH = 13.0 is $8.0 \times 10^{-4} \text{ s}^{-1}$, whereas k_{obs} in solution of 0.35 M carbonate buffer, $\alpha = 0.2$, is $1.1 \times 10^{-4} \text{ s}^{-1}$. Assuming that only the unprotonated form of the amino group reacts, this limiting rate is surpassed also at pH < 5 ($k_{\text{of}} = 3.2 \times 10^{-4} \text{ s}^{-1}$ at pH 4.5). These results clearly indicate the presence of parallel routes in the cyclization reaction to dioxopiperazine.

(b) The low value of the Brønsted coefficient ($\alpha = 0.54$) for the acid catalysis promoted by monofunctional acids indicates that this catalysis involves a proton transfer concerted with bond making and/or breaking.

(c) The enhanced reactivity observed with the polyfunctional acid catalysts bicarbonate and phosphate anions suggests that these anions take part in a proton switch step, as it is often observed in cases where such processes are involved.^{27,30}

(d) The shape of the Brønsted plot for the base catalysis suggests that this catalysis involves a simple proton transfer and thus probably acts on a step different from the acid-catalyzed step. The intermediate involved in the base catalysis has an acidic group with $\text{p}K_{\text{a}} \approx 7$.

(e) The shape of the pH rate profile at high pH values indicates either the formation of an ionizable intermediate, with a $\text{p}K_{\text{a}}$ value close to 13, or a change at this pH of the step which is rate determining.

(f) From the previous points, it emerges that the formation of **II** from **I** is a multistep process, which proceeds through more than one intermediate. The first is the trans \rightarrow cis isomerization of **I**, followed by intramolecular attack of the nitrogen atom on the carbonyl carbon. The positive value of the activation entropy ($29 \text{ J K}^{-1} \text{ mol}^{-1}$) determined in phosphate buffer suggests that neither of these two steps is rate-determining at neutral pH. Indeed, the ΔS^\ddagger for the trans \rightarrow cis isomerization has been estimated to be much lower,³¹ and that for the second step is expected to be negative, since the intramolecular attack yields a cyclic compound.³² It is worth noting that, for a multistep reaction in which the rate-limiting step is preceded by pre-equilibrium steps, the observed ΔS^\ddagger is the sum of the activation entropy of the rate-limiting step and of the entropy changes of the equilibrium steps.³³

(g) Finally, the dependence of k_{cat} and k_{cat}/f on α gives a clear indication that the buffers act only on the deprotonated form of the substrate.

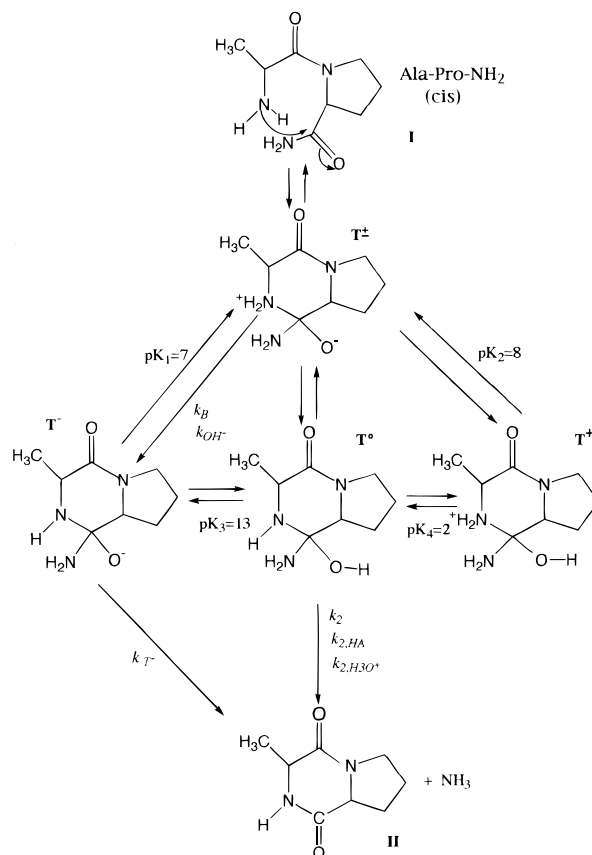


Figure 7. Proposed mechanism for the cyclization of H-Ala-Pro-NH₂ to the 2,5-dioxopiperazine.

Reaction Mechanism. A pathway for the formation of **II** from **I**, which fits the experimental data, is shown in Figure 7. The cis conformer with the amino group in the deprotonated state reacts by reversible intramolecular attack of the amino group on the carbonyl carbon giving the labile zwitterionic tetrahedral intermediate **T[±]**, which is in acid–base equilibrium with various forms characterized by different grades of protonation **T⁰**, **T⁺**, and **T⁻**. The $\text{p}K_{\text{a}}$ values of 7 and 13 for the equilibria $\text{T}^- + \text{H}^+ \rightleftharpoons \text{T}^\pm$ and $\text{T}^- + \text{H}^+ \rightleftharpoons \text{T}^0$ reported in the figure have been derived from the Brønsted plot for the base-catalysis and from the $\log(k_0) - \text{pH}$ plot, respectively. The last value agrees, within the experimental errors, with that calculated by the procedure of Fox and Jencks,¹⁶ using a recent estimation of the substituent constants.^{22,23,34} The $\text{p}K_{\text{a}}$ values for the equilibria $\text{T}^\pm + \text{H}^+ \rightleftharpoons \text{T}^+$ and $\text{T}^0 + \text{H}^+ \rightleftharpoons \text{T}^+$ cannot be derived from our experimental data, and the values of 8 and 2 reported in Figure 7 were obtained only through calculations.

The mechanism reported here implies that only the intermediates **T⁰** and **T⁻** pass directly to the product. The transformation of **T⁰** is general acid catalyzed: the acid protonates the poor leaving NH₂ group, facilitating the concerted breakdown of **T⁰** into the product. The base catalysts act on the deprotonation of **T[±]** to **T⁻**. At moderately basic pH and in absence of high concentration of base catalysts, the preferred pathway is $\text{T}^\pm \rightleftharpoons \text{T}^0 \rightarrow \text{product}$, with the second step being rate determining. An increase of the concentration of an efficient acid catalyst, such as the bifunctional bicarbonate anion, causes a change of the rate-determining step, from $\text{T}^0 \rightarrow \text{product}$ to the preceding step $\text{T}^\pm \rightleftharpoons \text{T}^0$. This pathway shows close analogy with that reported by Kirby and co-workers for the cyclization of methyl 3-(2-aminophenyl)propionate to the anilide.¹⁵ Both this reaction

(29) (a) Hand, E. S.; Jencks, W. P. *J. Am. Chem. Soc.* **1975**, *97*, 6221–6230. (b) Nagorski, R. W.; Mizerski, T.; Richard, J. P. *J. Am. Chem. Soc.* **1995**, *117*, 4718–4719.

(30) Kirby, A. J. *Adv. Phys. Org. Chem.* **1980**, *17*, 183.

(31) (a) Stain, R. L. *Adv. Prot. Chem.* **1993**, *44*, 1–24. (b) Hansch, C.; Leo, A.; Taft, R. W. *Chem. Rev.* **1991**, *91*, 165–195. (c) Green, D. V. S.; Hillier, I. H.; Morris, G. A.; Vhalley, L. *Magn. Res. Chem.* **1990**, *28*, 820–823.

(32) (a) Mandolini, L. *Bull. Soc. Fr.* **1988**, 173–176. (b) De Tar, D. F.; Luthra, N. P. *J. Am. Chem. Soc.* **1980**, *102*, 4505–4512. (c) Schlaeger, L. L.; Long, F. A. *Adv. Phys. Org. Chem.* **1963**, *1*, 1–33.

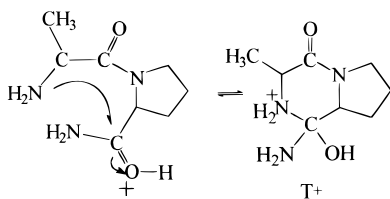
(33) Isaacs, N. S. *Physical Organic Chemistry*; Longman Scientific & Technical: New York, 1992; pp 77–113.

(34) Charton, M. *Prog. Phys. Org. Chem.* **1981**, *13*, 119–251.

and the reaction of **DKP** formation reported here involve a general acid catalysis of the rate-determining breakdown of a neutral tetrahedral intermediate. For both reactions, the catalysts phosphate and carbonate, because of the combination of acidic and basic groups, show enhanced reactivity.

In the formation of **DKP** at acidic pH, the high hydronium ion concentration favors the route $T^{\pm} \rightleftharpoons T^+ \rightleftharpoons T^0$, and the reaction rate becomes greater than the limiting value reached in carbonate buffer. The base catalysts, acting on the step T^{\pm} to T^- , make the parallel route $T^{\pm} \rightleftharpoons T^- \rightarrow \text{product}$ more favorable. The last step of this route is expected to have a very great kinetic constant k_{T^-} because of the negative charge on the oxygen atom of T^- (Figure 7). At pH 11, the hydroxide ion catalysis becomes increasingly important and explains the observed linear dependence of $\log(k_0)$ versus pH with unity slope (Figure 1). Moreover, as the pH approaches the pK_a for the dissociation of T^0 to T^- ($pK_a \approx 13$), the equilibrium shifts toward T^- and the observed rate constant increases more rapidly with the pH, because a conspicuous amount of the reactant can react through the route $T^{\pm} \rightleftharpoons T^0 \rightleftharpoons T^-$. As the $T^0 \rightleftharpoons T^-$ dissociation equilibrium is fully titrated, the parallel route adds a constant contribution to the reaction rate, and according to this kinetic model, $\log(k_0)$ is expected to resume the linear dependence on pH determined by the base-catalyzed pathway. The contribution of the parallel route can be estimated from the limiting value of k_{obs} reached at high concentration of carbonate buffer. The experimental data show an increase of k_0 of the magnitude expected from this kinetic model; however, at higher pH values the pH rate curve gradually levels off, indicating a further change of the rate-limiting step. For the trans \rightarrow cis isomerization of the peptide H-Ala-Pro-OCH₃, Grathwohl and Wüthrich²⁰ reported a rate constant of $5.8 \times 10^{-3} \text{ s}^{-1}$, similar in magnitude to the limiting value obtained in our study at high pH. On this basis, we propose that in this pH region the overall reaction rate is determined by the isomerization step.

At low pH, the constancy of k_0 is indicative of a hydronium ion-catalyzed reaction of the neutral form of the peptide or of the kinetically equivalent uncatalyzed reaction of a protonated form. It is well-known that the protonation of the carbonyl oxygen atom lowers the activation energy of the nucleophilic addition on the carbonyl carbon atom, making in many cases the direct formation of the cationic tetrahedral intermediate the preferred route at low pH.³⁵ Accordingly, a possible step for the cyclization to **DKP** is:



The ratio of O-protonated amide to N-protonated amine is given by the ratio of the corresponding acidity constants³⁶ and has an approximate value of 10^{-9} . The experiments reported here cannot exclude, because of the experimental error, that some amount of the substrate react through the O-protonated amide route. However, they clearly indicate the cyclization of the unprotonated form by general acid catalysis is the dominant route at low pH. Indeed, the data on buffer catalysis show that a general acid catalysis involves the unprotonated form of the substrate. Therefore, we would expect, at low pH values, H_3O^+ to catalyze the reaction of the unprotonated form, with a second-order rate constant [$k_{H_3O^+(\text{cal.})}$] of $55 \pm 45 \text{ M}^{-1} \text{ s}^{-1}$. This value has been derived from the coefficients of the straight line in the Brønsted plot for acid catalysis, computed without including the point for H_3O^+ and using $k_{H_3O^+} = -1.7$. The relatively large error is due to the low value of $k_{H_3O^+}$ in comparison with the pK_a values of the buffers used. The product " $k_{H_3O^+(\text{cal.})} \times [H_3O^+] \times f$ " gives the contribution to the observed rate constant for the H_3O^+ catalysis at low pH, and its value, $(9 \pm 7) \times 10^{-7} \text{ s}^{-1}$, is in satisfactory agreement with the k_0 value of $2.0 \times 10^{-7} \text{ s}^{-1}$, determined at low pH values by extrapolation at zero buffer concentration of the observed rate constant. In our opinion, the effect of the low concentration of the O-protonated amide form on the rate constant prevails over the activation effect of the proton on the oxygen atom.

Conclusion

The study of pH, buffer, and temperature effects on the cyclization reaction of H-Ala-Pro-NH₂ to **DKP** has produced a detailed description of the reaction pathway. The reaction proceeds through parallel routes, whose effectiveness depends on pH, and is characterized by changes of the rate-determining step with pH and buffer concentration. Our results provide new insights on the general mechanism of amino group addition to a carbonyl carbon atom, and underline the role played by the base and acid catalysis on the **DKP** formation. This is to be taken into account for the choice of the storage conditions and manipulation of peptides, which for their sequences are particularly prone to the cyclization reaction.

Acknowledgment. The authors thank Prof. A. J. Kirby for helpful discussions and Prof. P. Pucci and the staff of "Servizio di Spettrometria di Massa, Università C.N.R., Napoli" for providing the electrospray mass spectra. This work was supported by grants from the Italian "Ministero dell'Università e della Ricerca Scientifica e Tecnologica" and "Consiglio Nazionale delle Ricerche, Progetto Strategico di Biologia Strutturale".

JA972051A

(35) Kirby, A. J.; Lancaster, P. W. T. *G. J. Chem. Soc., Perkin Trans. 2* **1972**, 1206–1214.

(36) March, J. *Advanced Organic Chemistry*; John Wiley & Sons: New York, 1992; pp 248–272.